SUPPLEMENTAL DATA (Naschberger, Liebl et al.)

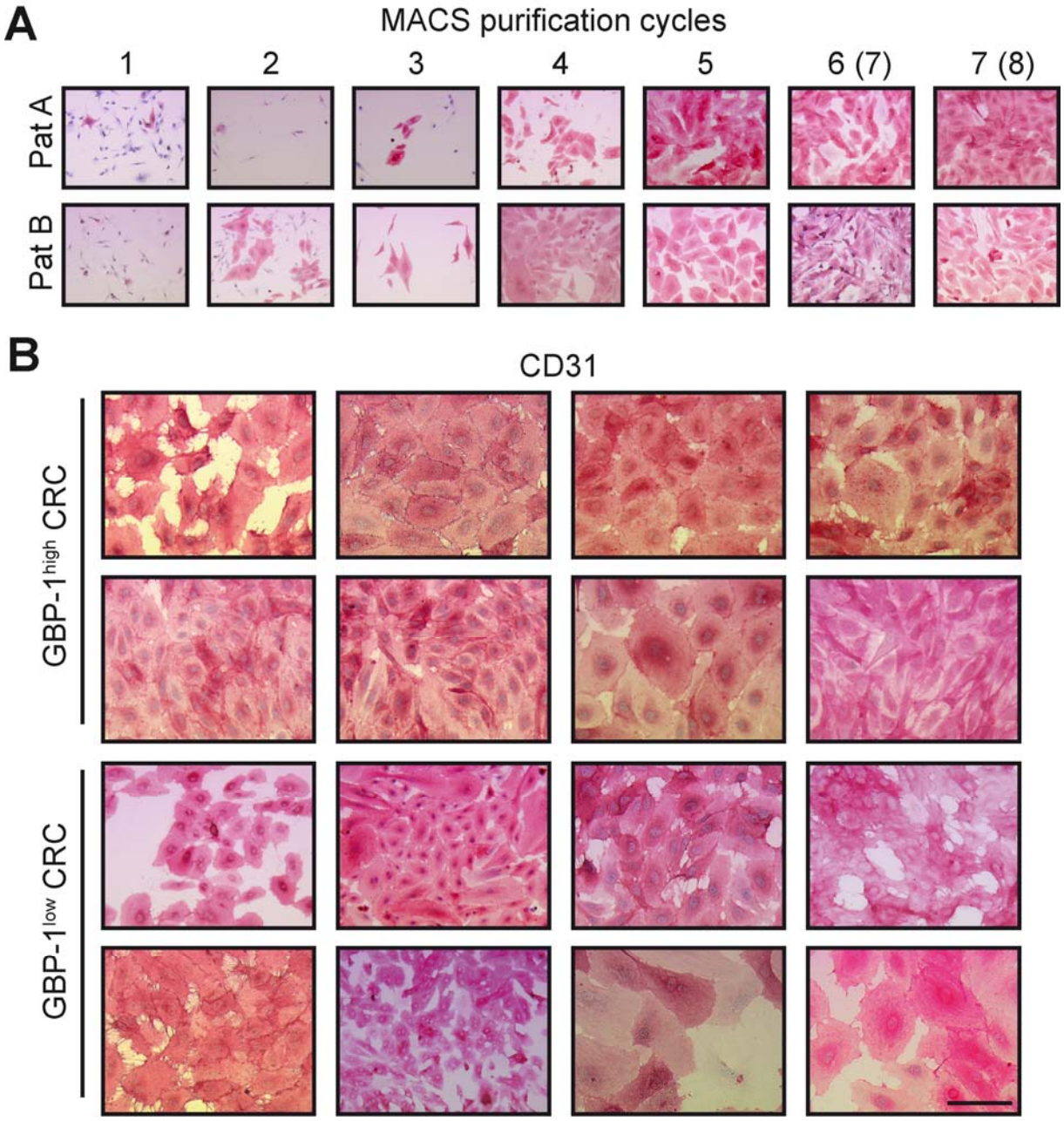

Supplemental Figure 1. CD31 staining of tumor endothelial cells isolated from colorectal carcinomas with GBP-1^{high} or GBP-1^{low} expression. (**A**) Enrichment and purity of tumor endothelial cells isolated from human colorectal carcinoma patients was monitored directly before and 24 hr after each MACS purification cycle by CD31 immunocytochemistry. Here, the results for two different patients after MACS purification are depicted as an example. MACS cycles in brackets are referring to patient A, without brackets to patient B. (**B**) Tumor endothelial cells were isolated from human colorectal carcinoma patients with either high (n=8) or low (n=8) GBP-1 expression in the tumor tissue. CD31 immunocytochemistry is depicted for all of the analyzed tumor endothelial cell cultures (n=16). Scale bar, 100 µm.

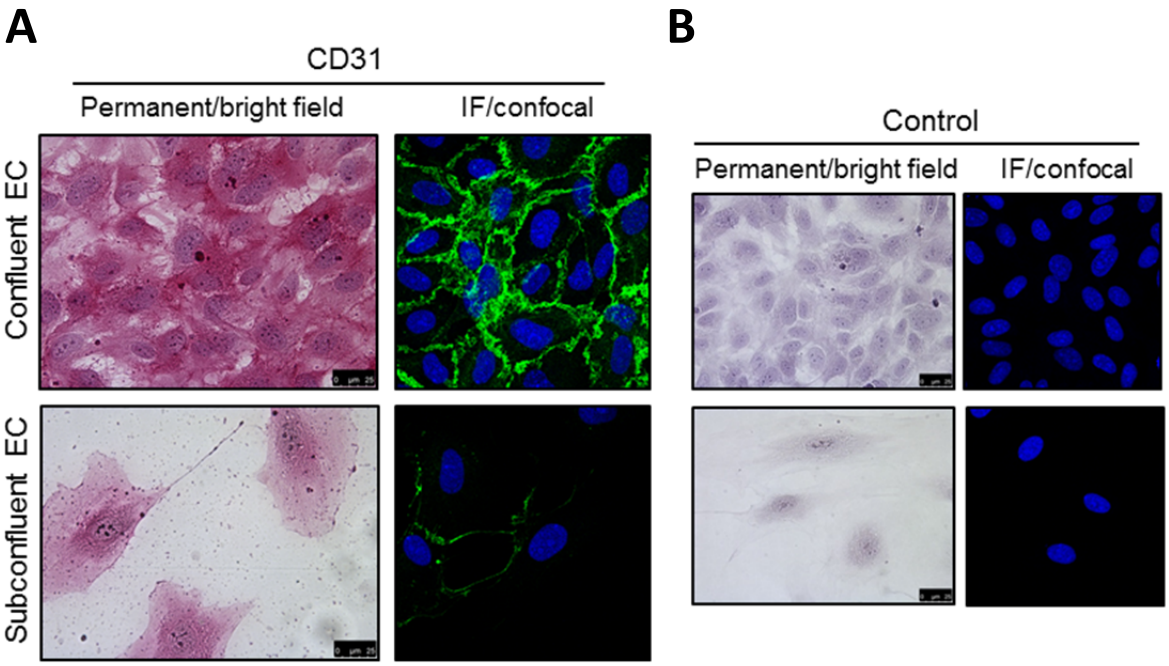

Supplemental Figure 2. Increased sensitivity of immunocytochemical staining of CD31 by permanent APAAP staining as compared to immunofluorescence resulting in different staining patterns. HUVEC were seeded at confluent and subconfluent densities and were immunocytochemically stained for **(A)** CD31 by permanent APAAP staining combined with bright field imaging as well as immunofluorescent (IF) staining followed by confocal imaging. **(B)** Negative controls for both stainings are depicted referring to a staining without the primary antibody. APAAP staining resulted in increased signal intensities in subconfluent cultures. Increased sensitivity resulted in staining of cytoplasmic CD31 which was not detected by the immunofluorescent staining procedure.

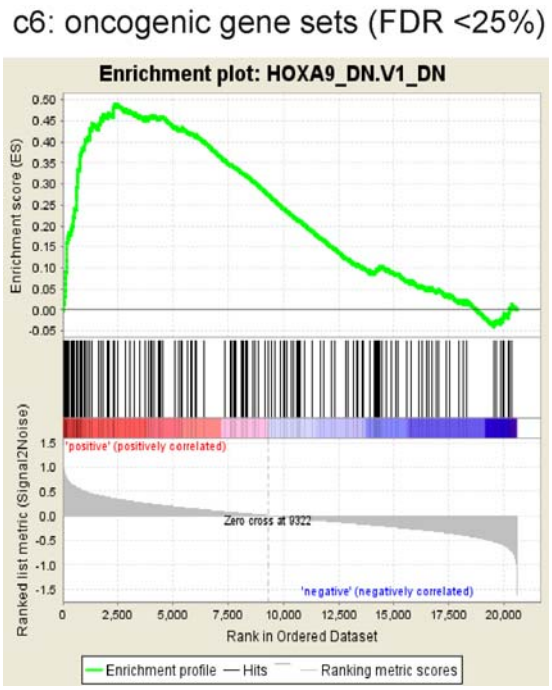

Supplemental Figure 3. Gene set enrichment plot of TEC transcriptomes from GBP-1^{high} compared to GBP-1^{low} CRC. RNA was isolated from TEC from GBP-1^{high} and GBP-1^{low} CRC, analyzed by hybridization to HG-U133-Plus 2.0 gene chips (Affymetrix) and gene set enrichment analysis (GSEA) was performed. The detailed lists of the identified features are given in Supplementary Table 4 and the enriched gene sets in Supplementary Table 5. The enrichment plot of the significantly enriched gene set HOXA9_DN.V1_DN (FDR of 0.073) associated with GBP-1^{high} TECs is depicted.

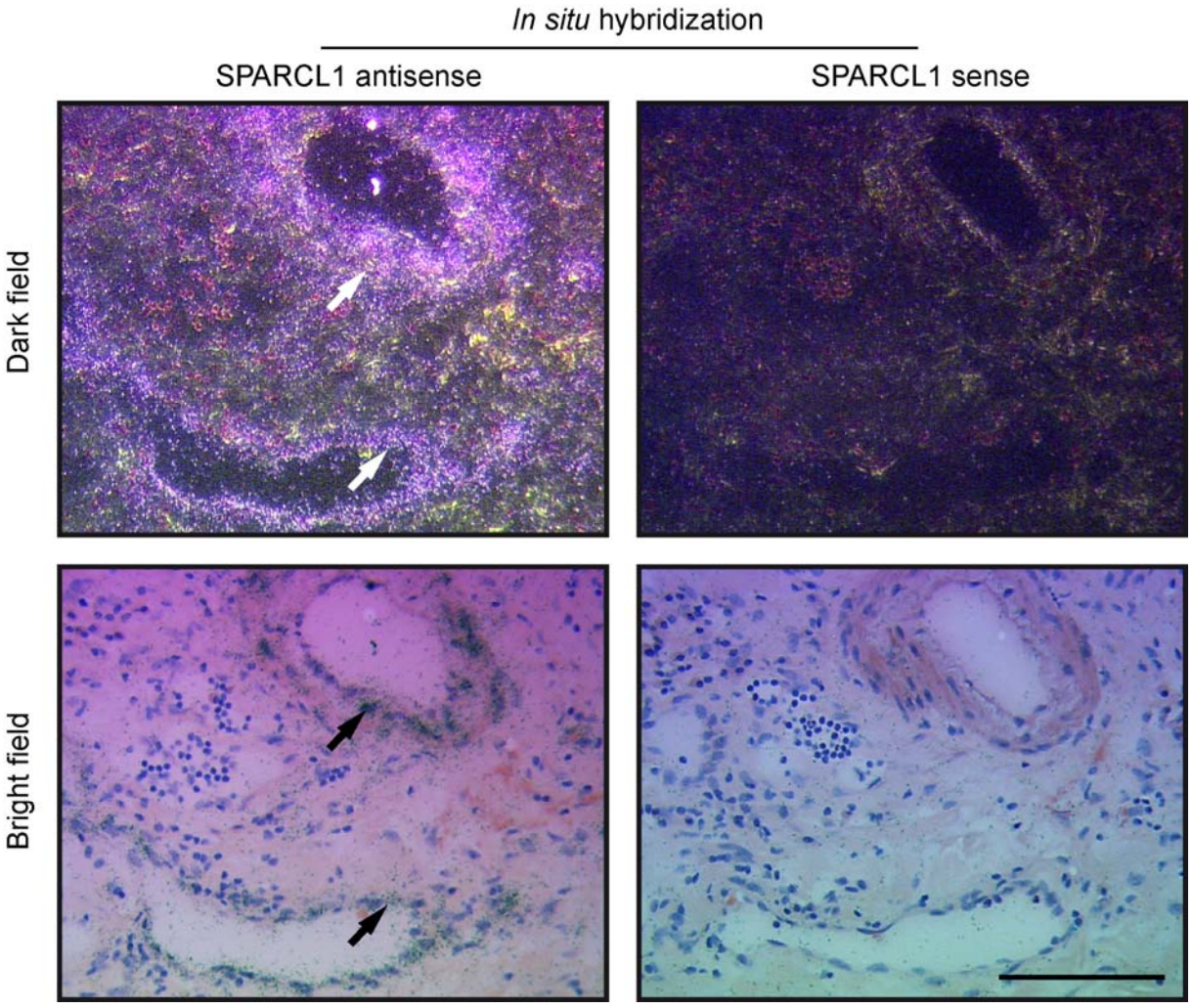

Supplemental Figure 4. SPARCL1 is expressed by vessels in colorectal carcinoma at the RNA level as detected by S^{35}-radioactive *in situ* hybridization. *In situ* hybridization on CRC tissue sections with SPARCL1-mRNA specific antisense and sense RNA probes was performed. Audioradiography signals appear in the bright field as black grains and in the dark field as white grains and are indicated by arrows. Scale bar, 100 µm.

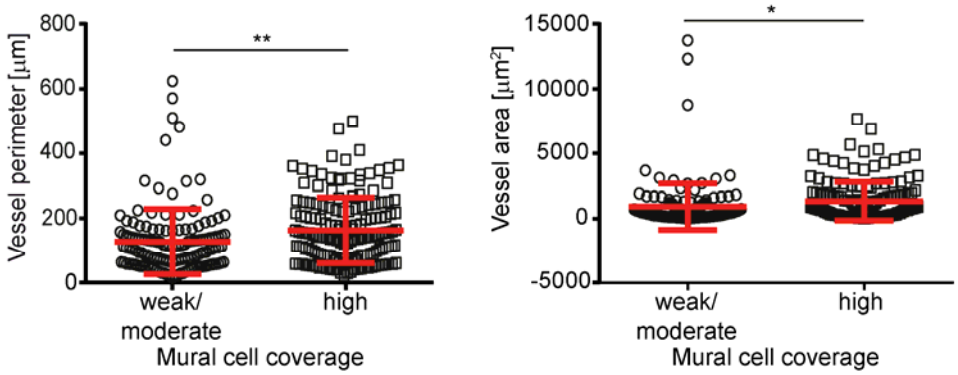

Supplemental Figure 5. Vessel size is significantly increased in vessels with high mural cell coverage. Vessel perimeters (left) and areas (right) were quantified for vessels evaluated in Fig. 7C. The vessel sizes are given in relation to weak/moderate and high mural cell coverage and are depicted as dot plot (red lines representing mean values and standard deviation). Statistical significances were determined by student's t-test (p-value *<0.05, **<0.01).

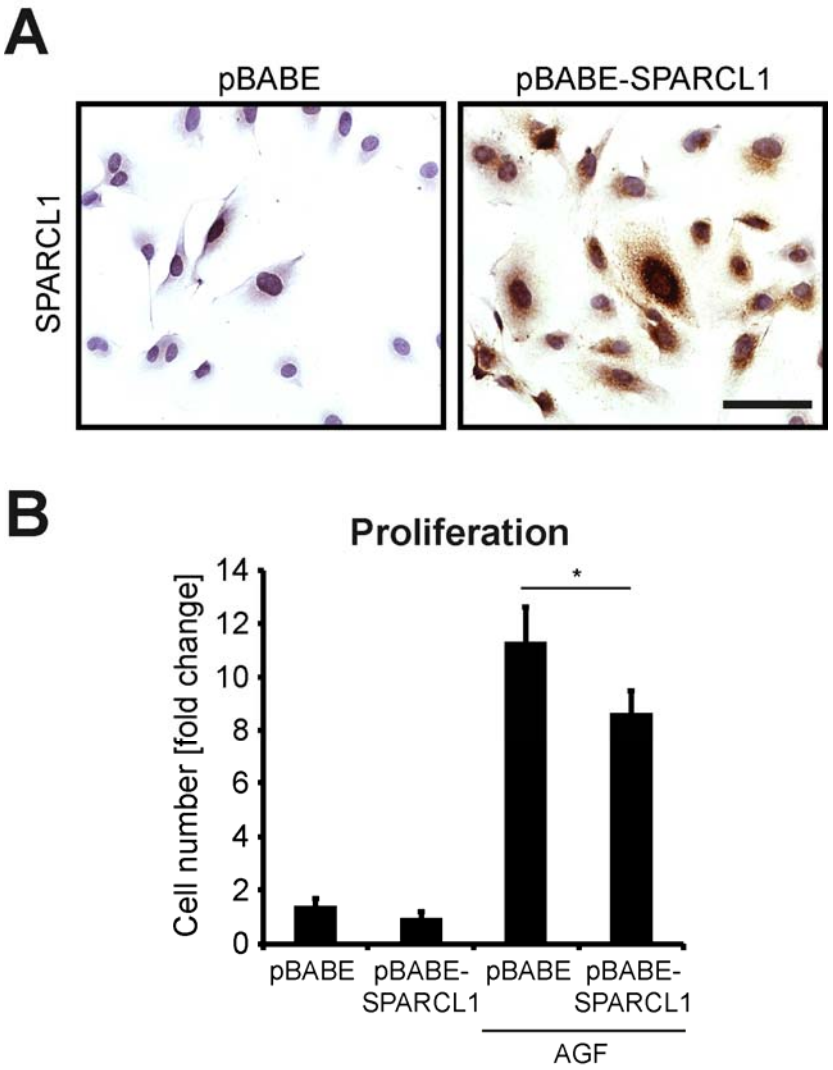

Supplemental Figure 6. Stable overexpression of SPARCL1 inhibits AGF-induced proliferation of EC. HUVEC were stably transduced by a retroviral SPARCL1-encoding vector (pBABE-SPARCL1) and the corresponding control vector (pBABE). (**A**) The cells were immunocytochemically stained for SPARCL1 expression (brown) and counterstained by hematoxylin (blue). Scale bar, 75 µm. (**B**). SPARCL1-transduced cells showed a significant inhibition of angiogenic growth factors (AGF=combined bFGF/VEGF, 10 ng/ml each)-induced proliferation by SPARCL1 (Student´s t-test).

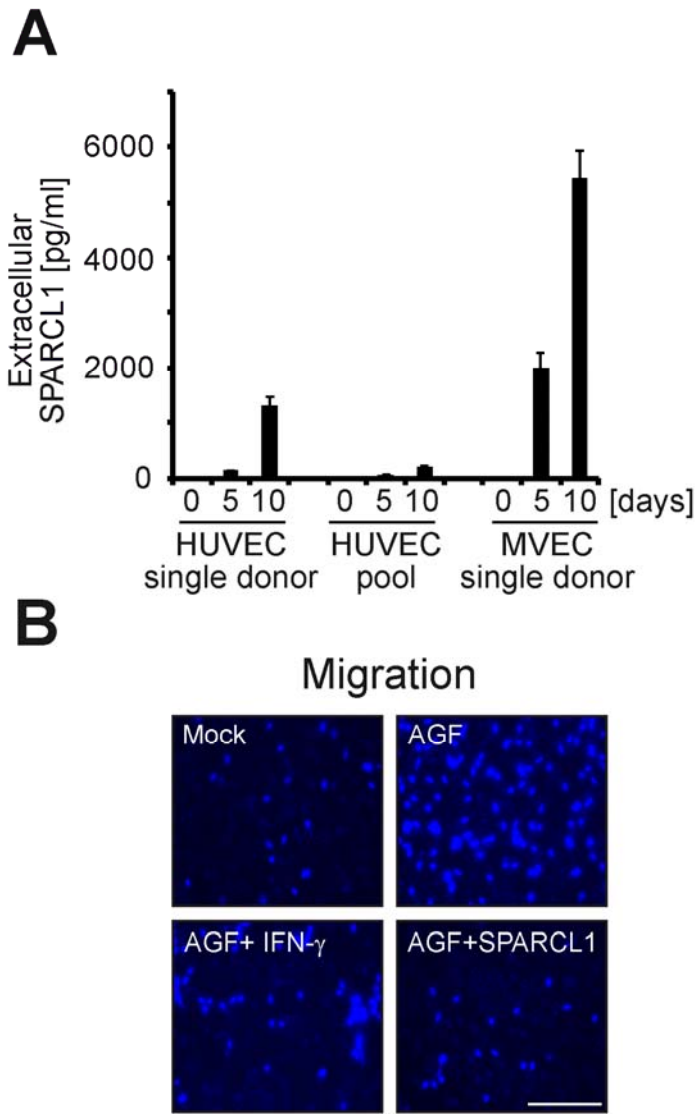

Supplemental Figure 7. SPARCL1 is secreted and inhibits migration of HUVEC. (**A**) Different cultures of HUVEC and MVEC were grown and at days 0, 5 and 10 conditioned media were harvested after 24 hr. Concentrations of secreted SPARCL1 were determined by SPARCL1-ELISA. (**B**) HUVEC were either untreated (mock) or treated with AGF (positive control), with AGF combined with IFN-γ (100 U/ml, negative control) or AGF with recombinant SPARCL1 (1.5 µg/ml). HUVECs were plated on transwell inserts, stimulated and analyzed after six hours. Migrated cells at the lower membrane side were determined by counterstaining with DAPI and representative images acquired by fluorescence microscopy are depicted (quantification compare Fig. 8D). Scale bar, 250 µm.

A

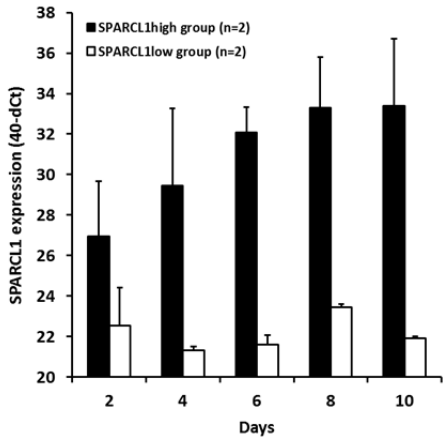

B

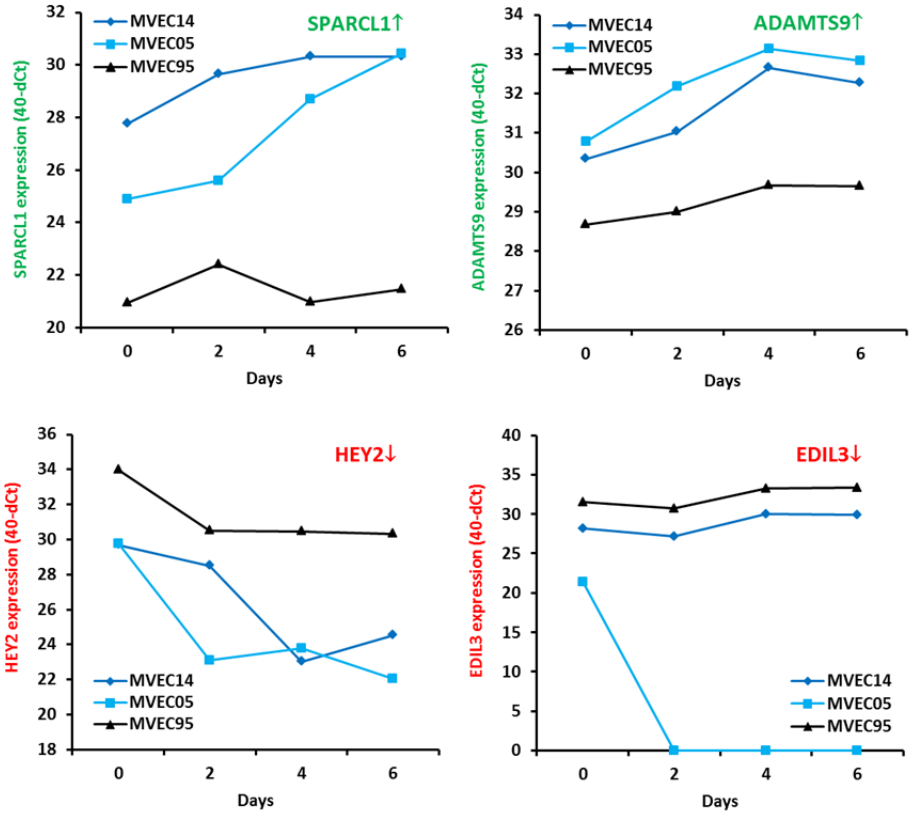

Supplemental Figure 8. Gene expression of SPARCL1, ADAMTS9, HEY2 and EDIL3 is consistently different between SPARCL1^{high} and SPARLC1^{low} EC during several days of cultivation. (**A**) SPARCL1^{high} (black, n=2) and SPARCL1^{low} (white, n=2) EC were seeded (day 0) and RNA extracts were harvested at the indicated time points. SPARCL1 mRNA expression levels were determined by RT-qPCR and the mean with standard deviation is depicted for each group. (**B**) SPARCL1^{high} (MVEC14 and MVEC05; blue rhombuses, light blue squares) and SPARCL1^{low} (MVEC95, black triangles) MVEC were seeded at the same cell density and RNA extracts were harvested at the indicated time points during 6 days. SPARCL1, ADAMTS9 (upregulated genes in TECs from GBP-1^{high} CRC) and HEY2, EDIL3 (downregulated genes in TECs from GBP-1^{high} CRC) RNA expression levels were determined by RT-qPCR. In all cases the differential gene expression between the groups was maintained.

Supplemental material and methods

Proliferation assays

EdU incorporation assay

Click-iT®EdU Alexa Fluor® 555 Imaging Kit (Life Technologies) was used to detect proliferating cells in transiently transfected EC. EdU was allowed to incorporate into the DNA of the cells for 2 hr. Afterwards, the cells were fixed with 10% formalin (neutral buffered, Sigma-Aldrich) for 10 min at RT and permeabilized for 30 min using 0.1% Triton-X (Sigma-Aldrich) in 1x PBS. The Click-iT reaction was performed according to the manufacturer's protocol.

Cell counting

HUVEC or SMC were seeded with a density of 3,000 cells/well in 24-well plates (for EC gelatin-coated) in the respective full medium (day 0). After 12 hr the medium was changed to low medium (basal medium with 0.5% FBS without supplements) for 12 hr. The cells were stimulated at day 1, 3 and 5, and the total cell number was determined at day 7 using a CASY TT cell counter (Schärfe Systems GmbH, Reutlingen, Germany). Each experiment was carried out in triplicates. The results are given as mean cell number with standard deviation.

Migration assays

Transmigration assay

HUVEC were seeded with $7.5x10^4$ cells/well, SMC with $1x10^5$ cells/well in 8 µm pore size Thincert cell culture inserts (Greiner, Frickenhausen, Germany) and put into 24 well-plates. HUVEC were stimulated for 6 hr (upper compartment), SMC for 4 hr (SMC: PDGF lower compartment, SPARCL1/IFN-γ upper compartment). Non-migrating cells were removed from the upper membrane with a swab. The cells were washed with 1xPBS and fixed with cold ethanol (4°C) for 24 hr. Nuclear staining was performed using DAPI (Life Technologies) for 10 min at RT and pictures of the membrane were acquired on a TCS SPE microscope (Leica). Cell numbers were determined by counting the total nuclei per optical field. All stimulations were performed in triplicates and five optical fields were counted per well. The results are given as mean cell number per optical field.

Scratch assay

MVEC were seeded with $3x10^4$ cells/cm^2 in gelatine-coated 4-well chamber slides (BD Biosciences) and were cultivated for 4 days. At day 5 the monolayer was scratched using a 10 µl pipette tip. The cells were washed two times with sterile PBS and then incubated in EGM2-MV full medium. Cells were harvested before scratching or 14/48 hr post scratch, fixed with 10% formalin (neutral buffered, Sigma-Aldrich) for 10 min. SMC scratch assay was performed by cultivating the cells in 6-well plates until confluency, followed by combined overnight starvation/stimulation and wounding/repeated stimulation of the cells with the indicated factors on the day after. Closure of the wound was quantified every 2 hr until 10 hr using TScratch software.

3D sprouting angiogenesis assay (spheroid assay)

Generation of spheroids: HUVEC (Promocell) were trypsinized and resuspended in ECGM containing 20% methocel. Methocel stock solution was prepared by dissolving 6 g carboxy-methylcellulose (Sigma-Aldrich) in 500 ml ECGM basal medium, cleared through centrifugation at 2,500 *x g*, 2 hr, RT and stored at 4°C. Spheroids were generated by the hanging drop method. To this goal, a cell suspension of 1.6 x 10^4 cells/ml was prepared and 500 drops with 25 µl volume were pipetted on a cell culture dish. The dish was turned upside down and the cells were incubated for 24 hr at 37°C and 5% CO_2. For harvesting spheroids were rinsed from the dishes using 1x PBS, collected in 50 ml tubes and centrifuged for 3 min at 500 *x g* at 20°C.

3D in vitro angiogenesis assay: to quantify the ability of spheroids to from sprouts after different treatments the spheroids were embedded in a collagen/methocel gel. The outer wells of a 24-well plate were filled with 1x PBS to avoid evaporation and the plates prewarmed in the incubator at 37°C. M199 (0.5 ml, 10x M199, Life Technologies) was mixed with 5 ml of rat tail collagen (Collagen R solution 0.2%, Serva, Heidelberg, Germany) and incubated on ice for at least 15 min. The harvested spheroid pellet was resuspendend in 5 ml FCS-containing methocel (20% FCS, 80% methocel). The medium-containing collagen was neutralized using cold 0.2 N NaOH until the pH-indicator turned from yellow to red. Neutralized collagen was carefully mixed with the spheroid-containing methocel and poured into the inner wells of the prewarmed 24 well plate (1 ml/well). Gels were incubated for 30 min to polymerize. The gels were overlayed with 100 µl ECGM basal medium containing the recombinant proteins for stimulation in a 10x concentration. Finally, the gels were incubated for 24 hr at 37°C, 5% CO_2 and were fixed with 10% formalin (neutral buffered, Sigma-Aldrich). Sprouts were evaluated acquiring pictures of 10 spheroids/well with a TCS SPE microscope (Leica). All stimulations were performed as duplicates. All sprouts were quantitatively measured using the LAS-AF software (Leica). The results are given as mean cumulative sprout length of 20 spheroids per stimulation.

Isolation of RNA from cell culture and human colon/CRC tissues

RNA from cells was isolated using the RNeasy mini kit (Qiagen). DNA digestion was performed as suggested by the manufacturer using the RNase-Free DNase Set (Qiagen). RNA quantity was determined using a Nanodrop 2000c (PeqLab, Erlangen, Germany). In all cases the standard protocols of the manufacturer were followed.

RNA isolation from human colon/CRC tissue: RNA was isolated using a fully automated extraction method from FFPE tissue (Tissue Preparation System with VERSANT Tissue Preparation Reagents, Siemens Healthcare Diagnostics, Tarrytown, NY) and has been described previously (1, 2). In brief, 10 µm paraffin sections (tumor content >30%) were directly subjected to automated total nucleic acid extraction. Samples were heat-lysed in 150 µl FFPE buffer at 80°C for 30 min with shaking. After cooling, enzymatic lysis was carried out at 65°C for 30 min with proteinase K. Any residual tissue debris was removed by nonspecific binding to silica-coated iron-oxide beads and subsequent magnetic separation. Deparaffinized and clarified lysates were transferred to new tubes and nucleic acids were bound to fresh silica-coated beads under chaotrophic conditions. Beads were washed 3 times and total nucleic acids were eluted with 100 µl of elution buffer at 70 °C followed by an automated DNase I digestion.

RT-qPCR

RT-qPCR primers and 5´-FAM-3´-TAMRA-labeled probes were designed using Primer Express 3.0 (Applied Biosystems, Carlsbad CA, USA) or PrimerBlast (NCBI). In case of multiple transcripts for one gene all of them were aimed to be targeted. All primers/probes were checked for specificity using BLAST (NCBI) and controlled for single nucleotide polymorphisms. Exon/intron junctions were spanned if possible. The primers and probes were purchased by Eurogentec (Serain, Belgium). The RNA primer/probe sequences were: CD105/endoglin (NM_001114753.2): forward GTGACATATACCACTAGCCAGGT, probe CGTGGCTCAGGCCCCCAATG, reverse CCAGGTGCCATTTTGCTTGG; CD31/PECAM-1 (NM_000442.4): GAGGTTCTGAGGGTGAAGGTGA, AGCCCCGGTGGATGAGGTCCAGA, TCCACCACCTTACTTGACAGGA; CD45/PTPRC (NM_002838.4): TGACTTCTCAGAGACCACAACTT, TCCACCCAAGTATCCCCGGACT, GTGAGGCGTCTGTACTGATGAA; CK-20 (NM_019010.2): AAAAGGAACTGAGGTTCAACTAAC, AGACGCACCTCCCAGAGCCT, TTGGCTAACTGGCTGCTGTAA; Desmin (NM_001927.3): GAGGAGAGCCGGATCAATCTC, ATCCAGACCTACTCTGCCCTCAACTTCCG, GGACCTCAGAACCCCTTTGC; GLB1 (SA-β-GAL, NM_000404.2): CGGGGTTCCTGGTTCGCAT, TGCGCAATGCCACCCAGAGG, CTTGAGGAAGGAGTCCCGGC; RPL37A (NM_000998.4): TGTGGTTCCTGCATGAAGACA, TGGCTGGCGGTGCCTGGA, GTGACAGCGGAAGTGGTATTGTAC; SPARCL1 (NM_001128310.1): GGAATTAAAGAAGAGGACATAGATGAA, TCAACTTTCCAGCATCCTCCTCTGTTCTAA, ATATAAATCTACAAGTATCACAGCTGCAT; VE-cadherin (NM_001795.3): ATGCGGCTAGGCATAGCATT, TCCATCCGCAGGACCAGTGACA, TGTGACTCGGAAGAACTGGC; vWF (NM_000552.3): TCTGTGGATTCAGTGGATGCA, CGCCAGGTCCAACAGAGTGACAGTGT, CGTAGCGATCTCCAATTCCAA. The DNA primer/probe sequences were: *PAEP* (gene ID 5047): CACAGAATGGACGCCATGAC, AAGCCCTCAGCCCTGCTCTCCATC, AAACCAGAGAGGCCACCCTAA. The SuperScript III Platinum One-Step Quantitative RT-PCR-System with ROX (Life Technologies) was used as recommended by the manufacturer except for a prolonged reverse transcription time of 30 min at 50°C. A reaction (10 µl total volume) consisted of 0.2 µl RT/Taq-mix, 50 nM ROX Reference Dye (Life Technologies), 10 ng total RNA, 500 nM forward/reverse primer each and 250 nM probe. The reactions were assayed in triplicates in 96-well-qPCR-plates (Agilent Technologies, Santa Clara, CA, USA) using a Mx3005P qPCR system (Agilent) together with the Versant kPCR software (Siemens Healthcare Diagnostics). For quantification of RNA samples the absence of residual DNA was analyzed by DNA-specific primers for the *progestagen-associated endometrial protein (PAEP)* gene and was in all cases negative. On each plate a commercial qPCR human reference total RNA (qRef, Agilent) was used as a positive control and a non-template control (NTC) as negative control. The fluorescence threshold (ROX dRn) was set to 0.02 for all samples. All samples were normalized using RPL37A (mean of triplicates) as a reference gene. Subsequently, the ΔΔCT-method was used for calculation of the respective fold changes for each target gene. The patient characteristics as analyzed by RT-qPCR are detailed in Supplementary Table 8.

Immunocytochemistry

Immunofluorescent cytochemistry

For SPARCL1, Ki-67 and IL-33 immunofluorescence detection microvascular ECs (MVEC) and human umbilical vein ECs (HUVEC) were seeded at a density of 30,000 cells/cm^2 and harvested after 12/24 hr (subconfluent) or 4/10/15/22 days (confluent). Subsequently, the cells were washed with PBS and fixed for 10 min at RT with 10% formalin (neutral buffered, Sigma-Aldrich, Munich, Germany). The cells were washed twice on a shaker with 0.45 µm

filtered TBS for 5 min, permeabilized using 0.1% Triton-X 100 (Sigma) in TBS for 30 min and blocked using 10% normal donkey serum (DNS, Vector Laboratories, Burlingame, CA, USA) in TBS for 10 min. Staining with primary antibodies was performed for 1 hr as follows: polyclonal goat anti-human SPARCL1 (R&D Systems, cat.no. AF2728, 0.4 µg/ml), monoclonal mouse anti-human IL-33 (Enzo Life Sciences, Lörrach, Germany, Nessy-1, 5 µg/ml) and monoclonal mouse anti-human Ki-67 (DakoCytomation, Hamburg, Germany, clone MIB-1, 7.2 µg/ml). Next, secondary antibodies (donkey anti-goat IgG Alexa 488, cat.no. A11055; donkey anti-mouse IgG Alexa 546, cat.no. A10036, Life Technologies, all 1:500) were incubated for 45 min on the slides and the nuclei were counterstained with DAPI (Life Technologies, 1:5,000). The slides were mounted using fluorescence mounting medium (DakoCytomation) and pictures were aquired using a DM6000 B epifluorescent or a TCS SP8 confocal microscope (Leica Microsystems GmbH, Wetzlar, Germany).

Permanent cytochemistry

CD31 permanent immunocytochemistry was performed as previously described (3, 4). Suspension cells (THP-1, Jurkat) were air dried in chamber slides and fixed overnight using 4°C ethanol. For SPARCL1 permanent immunocytochemistry the primary antibody (compare above) was detected using Vectastain Elite ABC-AP System (Vector Laboratories) and NovaRed substrate (Vector Laboratories). The slides were counterstained with Gill-III hematoxylin (Merck, Darmstadt, Germany), dehydrated and mounted with VectaMount permanent mounting medium (Vector Laboratories). The sections were analyzed using a DM6000 B microscope (Leica).

Immunohistochemistry

Immunofluorescent histochemistry

GBP-1 and CD31 immunohistochemistry was performed as previously described (5). The characteristics of the respective patients are detailed in Supplementary Table 7. Fluorescent immunohistochemistry was performed using formalin-fixed, paraffin-embedded tissue deparaffinized by xylene two times for 15 min. The tissue was rehydrated using decreasing concentrations of ethanol (100%, 96%, 85%, 70%) for 2 min each. Antigen retrieval was performed using Target Retrieval Solution (DakoCytomation), either at pH 9.0 (SPARCL1/CD31/α-SMA) or citrate at pH 6.0 (SPARCL1/CD31) at 95°C for 20 min followed by cooling for 20 min at RT. As a washing buffer between the incubation steps 0.45 µm filtered 1xTBS pH 7.6 was used. The slides were blocked by 10% DNS (Vector Laboratories) in TBS for 10 min. Next, the slides were incubated with the following primary antibodies in different combinations: polyclonal goat anti-human SPARCL1 antibody (R&D Systems, cat.no. AF2728, 4 µg/ml), monoclonal mouse anti-human CD31 (DakoCytomation, clone JC70A, 20.5 µg/ml) or polyclonal rabbit anti-human CD31 (Thermo Scientific, cat.no. RB-10333-P, 4 µg/ml), monoclonal mouse anti-human α-SMA (DakoCytomation, clone 1A4, 0.9 µg/ml), polyclonal goat anti-mouse SPARCL1 (R&D Systems, cat.no. AF2836, 2.5 µg/ml), monoclonal rat anti-mouse CD31 (Dianova, Hamburg, Germany, clone SZ31, 2 µg/ml) and monoclonal rabbit anti-mouse α-SMA (Abcam, Cambridge, United Kingdom, cat.no. ab124964, 0.128 µg/ml) as well as isotype controls normal goat IgG, normal rabbit IgG, normal mouse IgG1, and normal mouse IgG2A (all R&D Systems) in the same final concentrations as the respective detection antibodies in 5% DNS-TBS for 1 hr. Than the slides were incubated with the following secondary antibodies in different combinations: donkey anti-goat IgG Alexa 488 (cat.no. A11055), donkey anti-goat IgG Alexa 546 (cat.no. A11056), donkey anti-mouse IgG Alexa 647

(cat.no. A31571), donkey anti-rabbit IgG Alexa 546 (cat.no. A10040), donkey anti-rabbit IgG Alex 647 (cat.no. A31573, all Life Technologies, 1:500) and donkey anti-rat cross adsorbed IgG DyLight 488 (Thermo Scientific, cat.no. SA5-10026, 1:500) for 45 min. Nuclei were counterstained with Draq5 (Cell Signaling, Danvers, MA, USA, 1:800) or DAPI (Life Technologies, 1:5000) in water for 10 min and the slides were mounted with fluorescence mounting medium (DakoCytomation). Pictures were acquired using a TCS SP5 and SP8 confocal microscope (Leica).

Permanent histochemistry

For SPARCL1 permanent immunohistochemistry the staining was performed as described above with the following alterations: the polyclonal goat anti-human SPARCL1 antibody (R&D Systems, 0.5 µg/ml) as well as the isotype control normal goat IgG (R&D Systems, 0.5 µg/ml) were diluted in background reducing antibody diluent (DakoCytomation). The primary antibodies were detected using Vectastain Elite ABC-AP System (Vector Laboratories) and liquid permanent red (DakoCytomation, 30 min) as a substrate. The slides were counterstained with Gill-III hematoxylin (Merck), dehydrated and mounted with VectaMount permanent mounting medium (Vector Laboratories). The sections were analyzed using a DM6000 B microscope (Leica).

In situ hybridization

In situ hybridization with radioactively S^{35}-labeled *in vitro* transcribed RNA hybridization probes was performed as previously described (1, 6, 7). For generation of transcription plasmids a 676 bp cDNA fragment of the SPARCL1 sequence (NM_004684.5, bp 1841-2516) was inserted either in antisense and sense orientation in the pcDNA4/*Myc*-His B vector (Life Technologies). The patient characteristics as analyzed by immunohistochemical staining are detailed in Supplementary Table 7.

Quantification of cyto- and histochemical stainings

Microvessel density was quantified after CD31 immunohistochemical staining following standard protocols (8). In brief, for each tissue section/patient the vascular hot spot was determined and in these hot spots three optical fields (magnification 20x) were counted. Subsequently, average microvessel densities and standard deviations were calculated.

Vessel perimeter/area quantification was performed in ten vessels per patient (for patient characteristics see Supplementary Table 7, n=9 per group; n=270 total vessels) or mouse (n=21 mice [n=11 wild type, n=10 Sc1-/-] with n=10 vessels each; n=210 total vessels) with continuous CD31 expression and an obvious lumen. In the normal human colon, vessels located in the submucosa were quantified. The perimeters were determined with the analysis tool of the LAS-X software (Leica). Statistical differences were determined using unpaired student's t-test.

Relative SPARCL1 expression per vessel (SPARCL1 mosaic vessels) was determined by estimating the relative numbers of SPARCL1-expressing ECs compared to the total number of ECs constituting the respective vessel. The relative expression was categorized in four groups: 0-25%, 25-50%, 50-75%, 75-100%. All results were controlled by two independent investigators and discrepancies were discussed to obtain consent. The statistical significance of the relative distribution of SPARCL1 expression between the groups was determined by chi-square test.

The amount of α-SMA coverage per vessel was categorized in three groups: negative/weak, moderate and high. The statistical significance of the relative distribution of α-SMA coverage between the groups was determined by chi-square test.
The quantification of nuclear IL-33 and Ki-67 in all cell cultures was performed by counting the number of total nuclei as compared to nuclear IL-33-positive and Ki-67 positive cells with the LAS-AF software (Leica). Five pictures were acquired for each condition at a 20x magnification with approximately 100 nuclei per optical field. Results are given as ratio of nuclear IL-33/Ki67 positive nuclei per total nuclei per optical field.
The relative amount of proliferating cells in EC transiently transfected with SPARCL1 was determined by quantifying the relative percentage of EdU-positive cells in SPARCL1-positive compared to SPARCL1-negative cells using LAS X software (Leica). Pictures were acquired at a 20x magnification with approximately 100 nuclei per optical field and 13 pictures were evaluated. Results are given as ratio of EdU-positive cells per total SPARCL1-positive or SPARCL1-negative cells per optical field.

Supplemental Table 1. Clinical characteristics of the colorectal carcinoma patients included in the tumor endothelial cell isolation procedure for transcriptome analysis. The patients were differentiated using GBP-1 expression and were not different regarding their major clinical characteristics. UICC stage, localization of the tumor, neoadjuvant radio- or chemotherapy, grading, T-, N-, M-categories, L-, V-, R-classification, age and, sex are given for each patient. Chi square test and Mann-Whitney-U-test were used to analyze statistical differences (n.s.=not significant).

Pat	GBP-1 tissue	UICC stage	Localization	Neoadjuvant radio- or chemotherapy	Grading	T	N	M	L	V	R	Age	Sex
1	+	III	rectum	none	2	3	1	0	0	0	0	76	f
2	+	III	rectum	none	2	3	1	0	1	0	0	60	f
3	+	IV	ascending colon	none	3	3	2	1	1	1	2	23	f
4	+	II	sigmoid colon	none	3	4	0	0	0	1	0	65	m
5	+	II	transverse colon	none	2	3	0	0	0	0	0	61	m
6	+	I	rectum	none	2	2	0	0	0	0	0	49	f
7	+	I	transverse colon	none	2	2	0	0	0	0	0	70	f
8	+	II	colon left flexure	none	2	3	0	0	0	0	0	73	f
9	-	I	rectum	none	2	2	0	0	0	0	0	66	f
10	-	III	ascending colon	none	2	3	2	0	1	0	0	73	f
11	-	IV	ascending colon	none	2	3	2	1	1	0	2	70	f
12	-	I	rectum	none	2	2	0	0	0	0	0	56	m
13	-	II	sigmoid colon	none	2	3	0	0	0	0	0	57	f
14	-	III	transverse colon	none	3	4	2	0	0	0	0	53	f
15	-	II	rectum	none	2	3	0	0	0	0	0	44	m
16	-	I	rectum	none	1	2	0	0	0	0	0	68	f
p-value		**n.s.**		**n.s.**	**n.s.**	**n.s.**	**n.s.**	**n.s.**	**n.s.**	**n.s.**	**n.s.**	**n.s.**	**n.s.**

Supplemental Table 2. TECs isolated from human colorectal carcinoma show an endothelial cell phenotype. Expression levels of cell type-specific genes in tumor endothelial cells (TECs) and control cells (human umbilical vein endothelial cells [HUVEC], colorectal carcinoma cells [DLD-1], primary smooth muscle cells [SMC], primary dermal fibroblasts, monocytes [THP-1] and T-cells [Jurkat]) were determined using specific primer/probe sets with RT-qPCR using 10 ng total RNA. Results are given as mean values in 40-ΔCt. The measurements were performed in triplicates. n.d. = not detectable.

	CD31	vWF	CD105	VE-cadherin	CK-20	CD45	Desmin
TECs (n=7)	37.59	35.52	33.11	36.42	n.d.	n.d.	n.d.
HUVEC	39.09	38.12	35.92	37.49	n.d.	n.d.	n.d.
DLD-1	n.d.	n.d.	n.d.	n.d.	24.76	n.d.	19.47
SMC	n.d.	n.d.	34.56	32.15	n.d.	n.d.	20.01
Fibroblasts	n.d.	n.d.	34.14	n.d.	n.d.	n.d.	30.08
THP-1	35.91	n.d.	32.23	n.d.	n.d.	34.72	24.43
Jurkat	33.22	n.d.	n.d.	n.d.	n.d.	33.48	n.d.

Supplemental Table 3. Sensitivity analysis of the RT-qPCR approach for the detection of cross-contaminating cell types in endothelial cells. HUVEC were mixed with other cell types (indicated) in the relative amounts as given below after automated cell count (final total amount of cells $3x10^4$) directly before cell harvesting. RNA was extracted and subjected to RT-qPCR analysis. Pure HUVEC (first lane) were used as a control. The limits of detection for each cell type (2% DLD, 1% NHDF, 1% SMC, 0.1% Jurkat, 0.5% THP-1) are shaded in grey. The indicated values are the mean values given as 40-ΔCt. Abbreviations: human umbilical vein endothelial cells, HUVEC; human colorectal carcinoma cell line, DLD-1; primary normal human dermal fibroblasts, NHDF; primary smooth muscle cells, SMC; T-cell line, Jurkat; monocytic cell line, THP-1. n.d.= not detectable.

Sample	CD31	CD45	Desmin	CK20
HUVEC	37.21	n.d.	n.d.	n.d.
5% DLD-1	37.10			19.03
3% DLD-1	37.21			18.88
2% DLD-1	37.10			19.28
1% DLD-1	37.34			n.d.
0.5% DLD-1	36.13			n.d.
0.1% DLD-1	37.19			n.d.
1% NHDF	36.99		20.94	
0.5% NHDF	37.12		n.d.	
0.1% NHDF	36.85		n.d.	
3% SMC	36.99		19.00	
2% SMC	37.40		20.75	
1% SMC	37.43		20.03	
0.5% SMC	37.08		n.d.	
0.1% SMC	37.01		n.d.	
1% Jurkat	37.18	25.15		
0.5% Jurkat	37.51	24.13		
0.1% Jurkat	36.99	21.37		
1% THP-1	37.37	22.07		
0.5% THP-1	36.93	20.78		
0.1% THP-1	37.02	n.d.		

Supplemental Table 4. Top 50 features identified by gene set enrichment analysis (GSEA) after transcriptome analysis of tumor endothelial cells isolated from GBP-1^{high} compared to GBP-1^{low} colorectal carcinomas.

Name	Gene title	Score
GALK1	galactokinase 1	1.439
ATN1	atrophin 1	1.361
LOC647323	-	1.357
CALR	calreticulin	1.287
TUBB2A /// TUBB2B	null	1.237
RAB11B	RAB11B, member RAS oncogene family	1.180
FGF12	fibroblast growth factor 12	1.162
PPARGC1B	peroxisome proliferative activated receptor, gamma, coactivator 1, beta	1.138
TLN1	talin 1	1.135
LOC643287	-	1.119
DCAMKL3	doublecortin and CaM kinase-like 3	1.108
USHBP1	Usher syndrome 1C binding protein 1	1.092
LOC196463	-	1.084
PRKAG2	protein kinase, AMP-activated, gamma 2 non-catalytic subunit	1.082
VAMP2	vesicle-associated membrane protein 2 (synaptobrevin 2)	1.079
LOC339788	-	1.077
RASGEF1B	RasGEF domain family, member 1B	1.069
SLC9A3R2	solute carrier family 9 (sodium/hydrogen exchanger), member 3 regulator 2	1.066
PPM1G	protein phosphatase 1G (formerly 2C), magnesium-dependent, gamma isoform	1.062
ACR	acrosin	1.056
SORBS3	sorbin and SH3 domain containing 3	1.054
RAP2A /// RAP2B	null	1.047
SREBF2	sterol regulatory element binding transcription factor 2	1.036
C10ORF55	chromosome 10 open reading frame 55	1.022
LOC399884	-	1.021
PGR	progesterone receptor	1.021
RAB5C	RAB5C, member RAS oncogene family	1.020
ATXN2L	ataxin 2-like	1.016
LOC284912	-	1.009
PKN1	protein kinase N1	1.004
FLJ44894	-	0.996
EYA3	eyes absent homolog 3 (Drosophila)	0.996
TPMT	thiopurine S-methyltransferase	0.996
LASS4	LAG1 homolog, ceramide synthase 4 (S. cerevisiae)	0.996
BAHD1	bromo adjacent homology domain containing 1	0.986
VEGFB	vascular endothelial growth factor B	0.982
FHOD1	formin homology 2 domain containing 1	0.975
TPM3 /// TPM4	null	0.974
YWHAE	tyrosine 3-monooxygenase/tryptophan 5-monooxygenase activation protein, epsilon polypeptide	0.967
IL3RA	interleukin 3 receptor, alpha (low affinity)	0.964
FAM120C	family with sequence similarity 120C	0.963
ZBTB40	zinc finger and BTB domain containing 40	0.962
STRN	striatin, calmodulin binding protein	0.962
C6ORF106	chromosome 6 open reading frame 106	0.955
TRIM65	tripartite motif-containing 65	0.952
SR-A1	-	0.949
LATS1	LATS, large tumor suppressor, homolog 1 (Drosophila)	0.948
C11ORF42	chromosome 11 open reading frame 42	0.944
FASN	fatty acid synthase	0.943
LOC202347	-	0.939
LOC474170	-	-0.903
USH3A	Usher syndrome 3A	-0.904
GNRH2	gonadotropin-releasing hormone 2	-0.905
ALPP /// ALPPL2	null	-0.905
SERPINA6	serpin peptidase inhibitor, clade A (alpha-1 antiproteinase, antitrypsin), member 6	-0.910
CDC2L5	cell division cycle 2-like 5 (cholinesterase-related cell division controller)	-0.910
FLJ30092	-	-0.921
AP1S1	adaptor-related protein complex 1, sigma 1 subunit	-0.921

ZNF777	zinc finger protein 777	-0.922
LOC642775	null	-0.927
FLJ31438	-	-0.928
TMEM10	transmembrane protein 10	-0.932
HYMAI	hydatidiform mole associated and imprinted	-0.935
ATM	ataxia telangiectasia mutated (includes complementation groups A, C and D)	-0.936
NFE2	nuclear factor (erythroid-derived 2), 45kDa	-0.936
SLC5A2	solute carrier family 5 (sodium/glucose cotransporter), member 2	-0.940
FBXW12	F-box and WD-40 domain protein 12	-0.940
FLJ37538	-	-0.944
MAFF	v-maf musculoaponeurotic fibrosarcoma oncogene homolog F (avian)	-0.949
FLJ22795	-	-0.953
DNAI1	dynein, axonemal, intermediate chain 1	-0.954
STAT4	signal transducer and activator of transcription 4	-0.962
OPRD1	opioid receptor, delta 1	-0.962
TMEM163	transmembrane protein 163	-0.966
DST	dystonin	-0.972
MGC3032	-	-0.972
PHOX2B	paired-like homeobox 2b	-0.974
PRKXP1	protein kinase, X-linked, pseudogene 1	-0.983
FLJ34306	-	-0.987
C1ORF53	chromosome 1 open reading frame 53	-0.993
LOC165186	-	-1.004
AATK	apoptosis-associated tyrosine kinase	-1.004
TBC1D3 /// TBC1D3C /	null	-1.043
HMP19	-	-1.056
LOC150527	-	-1.073
WNT9A	wingless-type MMTV integration site family, member 9A	-1.078
FLJ30307	-	-1.086
C21ORF104	chromosome 21 open reading frame 104	-1.096
LOC644541 /// LOC649	null	-1.097
CNIH2	cornichon homolog 2 (Drosophila)	-1.099
ALF	-	-1.121
EPHB3	EPH receptor B3	-1.146
C9ORF152	chromosome 9 open reading frame 152	-1.151
C9ORF64	chromosome 9 open reading frame 64	-1.170
PRSS16	protease, serine, 16 (thymus)	-1.178
C12ORF50	chromosome 12 open reading frame 50	-1.250
SLC6A12	solute carrier family 6 (neurotransmitter transporter, betaine/GABA), member 12	-1.287
KCNJ10	potassium inwardly-rectifying channel, subfamily J, member 10	-1.402
TRIM46	tripartite motif-containing 46	-1.454
MGC50811	-	-1.612

Supplemental Table 5. Gene sets enriched between tumor endothelial cells isolated from GBP-1^{high} and GBP-1^{low} colorectal carcinomas as identified by GSEA. Enriched gene sets were analyzed for all 7 major collections deposited in the molecular signatures database v4.0. Enriched gene sets are given if FDR <25% or NOM p-val <0.01. Abbreviations: false discovery rate (FDR), nominal p-value (NOM p-val), enrichment score (ES), normalized enrichment score (NES), familywise-error rate (FWER).

	Enriched genes sets (FDR<25%)	Enriched gene sets (NOM p-val<0.01)	NAME	SIZE	ES	NES	NOM p-val	FDR q-val	FWER p-val	RANK AT MAX	LEADING EDGE
c1: positional gene sets	0 (positive)	0 (positive)	-								
	0 (negative)	0 (negative)	-								
c2: curated gene sets	0 (positive)	14 (positive)	CREIGHTON_AKT1_SIGNALING_VIA_MTOR_UP	32	0.560	1.943	0.000	0.490	0.272	2527	tags=31%, list=12%, signal=36%
			BIOCARTA_IL3_PATHWAY	15	0.658	1.818	0.000	0.954	0.718	3088	tags=53%, list=15%, signal=63%
			HWANG_PROSTATE_CANCER_MARKERS	26	0.576	1.842	0.002	0.902	0.625	2296	tags=31%, list=11%, signal=35%
			BIOCARTA_CHREBP2_PATHWAY	42	0.547	1.958	0.002	0.794	0.240	3218	tags=40%, list=16%, signal=48%
			CAIRO_PML_TARGETS_BOUND_BY_MYC_UP	23	0.678	1.862	0.002	0.940	0.552	3581	tags=52%, list=17%, signal=63%
			HONRADO_BREAST_CANCER_BRCA1_VS_BRCA2	18	0.657	1.800	0.004	0.985	0.788	1929	tags=56%, list=9%, signal=61%
			VIETOR_IFRD1_TARGETS	19	0.677	1.771	0.006	0.883	0.860	3943	tags=58%, list=19%, signal=72%
			PID_S1P_S1P3_PATHWAY	25	0.568	1.775	0.008	1.000	0.848	4133	tags=56%, list=20%, signal=70%
			TIMOFEEVA_GROWTH_STRESS_VIA_STAT1_DN	15	0.597	1.671	0.008	1.000	0.978	2091	tags=47%, list=10%, signal=52%
			BIOCARTA_HER2_PATHWAY	22	0.469	1.681	0.008	1.000	0.976	3088	tags=27%, list=15%, signal=32%
			SIG_PIP3_SIGNALING_IN_B_LYMPHOCYTES	34	0.457	1.581	0.010	0.787	1.000	2859	tags=32%, list=14%, signal=38%
			CUI_GLUCOSE_DEPRIVATION	57	0.379	1.504	0.010	0.775	1.000	1592	tags=19%, list=8%, signal=21%
			BIOCARTA_ECM_PATHWAY	23	0.615	1.775	0.010	0.954	0.849	4099	tags=48%, list=20%, signal=60%
			REACTOME_DOWNSTREAM_SIGNAL_TRANSDUCTION	84	0.361	1.560	0.010	0.795	1.000	3826	tags=35%, list=19%, signal=42%
	0 (negative)	4 (negative)	SU_PANCREAS	47	-0.442	-1.585	0.002	1.000	0.999	5234	tags=43%, list=25%, signal=57%
			REACTOME_SIGNALING_BY_BMP	21	-0.551	-1.639	0.002	1.000	0.994	3897	tags=48%, list=19%, signal=59%
			TIEN_INTESTINE_PROBIOTICS_6HR_DN	141	-0.341	-1.566	0.004	1.000	0.999	6046	tags=43%, list=29%, signal=61%
			REACTOME_DOWNREGULATION_OF_SMAD2_3_SMAD4_ TRANSCRIPTIONAL_ACTIVITY	17	-0.448	-1.693	0.004	1.000	0.974	976	tags=24%, list=5%, signal=25%
c3: motif gene sets	0 (positive)	0 (positive)	-								
	0 (negative)	4 (negative)	V$NFAT_Q4_01	234	-0.302	-1.429	0.002	1.000	0.948	3087	tags=23%, list=15%, signal=27%
			ACATATC,MIR-190	52	-0.430	-1.677	0.006	1.000	0.371	3015	tags=31%, list=15%, signal=36%
			GTTAAAG,MIR-302B	56	-0.428	-1.657	0.006	0.674	0.426	3888	tags=34%, list=19%, signal=42%
			TACTTGA,MIR-26A,MIR-26B	262	-0.387	-1.628	0.008	0.568	0.498	4441	tags=35%, list=22%, signal=44%
c4: computational gene sets	0 (positive)	0 (positive)	-								
	0 (negative)	3 (negative)	MODULE_237	49	-0.417	-1.636	0.004	0.828	0.819	2477	tags=27%, list=12%, signal=30%
			GCM_ZNF198	97	-0.361	-1.701	0.004	1.000	0.656	5613	tags=40%, list=27%, signal=55%
			GCM_RAB10	142	-0.409	-1.829	0.006	1.000	0.303	6437	tags=51%, list=31%, signal=73%
c5: GO gene sets	1 (positive)	3 (positive)	HYDROLASE_ACTIVITY_ACTING_ON_CARBON_NITROGEN_ NOT_PEPTIDEBONDSIN_LINEAR_AMIDES	19	0.616	1.936	0.004	0.206	0.098	247	tags=21%, list=1%, signal=21%
			GENERAL_RNA_POLYMERASE_II_TRANSCRIPTION_FACTOR _ACTIVITY	24	0.492	1.813	0.000	0.555	0.351	1290	tags=21%, list=6%, signal=22%
			HYDROLASE_ACTIVITY_ACTING_ON_CARBON_NITROGEN_	19	0.616	1.936	0.004	0.206	0.098	247	tags=21%, list=1%, signal=21%

			NOT_PEPTIDEBONDSIN_LINEAR_AMIDES								
			BASE_EXCISION_REPAIR	15	0.657	1.673	0.004	1.000	0.799	2182	tags=53%, list=11%, signal=60%
	0 (negative)	2 (negative)	SYNAPSE_ORGANIZATION_AND_BIOGENESIS	22	-0.650	-1.724	0.000	1.000	0.624	2526	tags=41%, list=12%, signal=47%
			SYNAPTOGENESIS	18	-0.701	-1.741	0.002	1.000	0.561	2447	tags=44%, list=12%, signal=50%
c6: oncogenic gene sets	1 (positive)	1 (positive)	HOXA9_DN.V1_DN	166	0.489	1.751	0.004	0.073	0.076	2329	tags=34%, list=11%, signal=38%
			HOXA9_DN.V1_DN	166	0.489	1.751	0.004	0.073	0.076	2329	tags=34%, list=11%, signal=38%
	0 (negative)	1 (negative)	TGFB_UP.V1_DN	174	-0.364	-1.499	0.006	1.000	0.593	5377	tags=42%, list=26%, signal=56%
c7: immunologic signatures	0 (positive)	0 (positive)	-								
	0 (negative)	6 (negative)	GSE17974_CTRL_VS_ACT_IL4_AND_ANTI_IL12_48H_CD4_TCELL_UP	151	-0.375	-1.554	0.002	1.000	0.786	4412	tags=32%, list=21%, signal=41%
			GSE29615_CTRL_VS_DAY3_LAIV_IFLU_VACCINE_PBMC_DN	143	-0.365	-1.647	0.002	1.000	0.538	4916	tags=38%, list=24%, signal=49%
			GSE15659_CD45RA_NEG_CD4_TCELL_VS_NONSUPPRESSIVE_TCELL_UP	142	-0.357	-1.508	0.002	1.000	0.871	4254	tags=33%, list=21%, signal=41%
			GSE24634_NAIVE_CD4_TCELL_VS_DAY7_IL4_CONV_TREG_UP	157	-0.372	-1.605	0.004	1.000	0.664	4228	tags=34%, list=21%, signal=42%
			GSE17721_CPG_VS_GARDIQUIMOD_24H_BMDM_DN	170	-0.356	-1.559	0.004	1.000	0.779	5515	tags=42%, list=27%, signal=57%
			GSE9006_HEALTHY_VS_TYPE_2_DIABETES_PBMC_AT_DX_DN	166	-0.380	-1.562	0.008	1.000	0.772	5319	tags=42%, list=26%, signal=56%

Supplemental Table 6. Top 50 up- and top 50 downregulated target genes in tumor endothelial cells isolated from GBP-1^{high} versus GBP-1^{low} colorectal carcinoma as identified by significance analysis of microarray (SAM). Top 50 up- and downregulated target genes identified by SAM with fold change >2-fold. Redundant genes with different probe set IDs are shaded in grey. False discovery rate (FDR, q-value %), Probe set IDs (Affymetrix) and RefSeq protein and transcript IDs are given for each of the identified targets. If multiple protein or transcript IDs were annotated the first is listed.

Fold-induction	FDR (q-value %)	Gene Symbol	Gene Title	Probe Set ID	RefSeq Protein ID	RefSeq Transcript ID
34.038	12.17	SPARCL1	SPARC-like 1 (hevin)	200795_at	NP_001121782	NM_001128310
7.889	0.00	PPP1R14A	protein phosphatase 1, regulatory (inhibitor) subunit 14A	227006_at	NP_001230876	NM_001243947
7.486	2.49	SEPT9	septin 9	207425_s_at	NP_001106963	NM_001113491
5.924	5.81	GPAT2	glycerol-3-phosphate acyltransferase 2, mitochondrial	235557_at	NP_997211	NM_207328
5.570	3.89	SLC9A3R2	solute carrier family 9, subfamily A (NHE3, cation proton antiporter 3), member 3 regulator 2	209830_s_at	NP_001123484	NM_001130012
5.292	7.24	NEURL1B	neuralized homolog 1B (Drosophila)	225355_at	NP_001136123	NM_001142651
5.248	2.63	CALR	calreticulin	214315_x_at	NP_004334	NM_004343
4.415	4.68	ACE	angiotensin I converting enzyme (peptidyl-dipeptidase A) 1	209749_s_at	NP_000780	NM_000789
4.115	5.81	INF2	inverted formin, FH2 and WH2 domain containing	222534_s_at	NP_001026884	NM_001031714
4.111	16.54	MYRIP	myosin VIIA and Rab interacting protein	214156_at	NP_056275	NM_015460
4.031	4.68	FAM65A	family with sequence similarity 65, member A	230806_s_at	NP_001180451	NM_001193522
3.942	2.63	KAT6A/MYST3	K(lysine) acetyltransferase 6A/MYST3	216361_s_at	NP_001092882	NM_001099412
3.875	0.00	ATN1	atrophin 1	40489_at	NP_001007027	NM_001007026
3.851	0.00	MAZ	MYC-associated zinc finger protein (purine-binding transcription factor)	207824_s_at	NP_001036004	NM_001042539
3.830	7.90	MEOX2	mesenchyme homeobox 2	206201_s_at	NP_005915	NM_005924
3.797	2.63	CALR	calreticulin	212953_x_at	NP_004334	NM_004343
3.690	2.63	ADAMTS9	ADAM metallopeptidase with thrombospondin type 1 motif, 9	1554697_at	NP_891550	NM_182920
3.639	2.63	DYRK1A	dual-specificity tyrosine-(Y)-phosphorylation regulated kinase 1A	211079_s_at	NP_001387	NM_001396
3.594	4.52	CNOT6L	CCR4-NOT transcription complex, subunit 6-like	1553267_a_at	NP_653172	NM_144571
3.570	17.73	TCF3	Transcription factor 3 (E2A immunoglobulin enhancer binding factors E12/E47)	202648_at	NP_001129611	NM_001136139
3.567	0.00	ATN1	atrophin 1	208871_at	NP_001007027	NM_001007026
3.535	2.63	ARHGDIA	Rho GDP dissociation inhibitor (GDI) alpha	213606_s_at	NP_001172006	NM_001185077
3.396	2.63	CAMK2N1	calcium/calmodulin-dependent protein kinase II inhibitor 1	228302_x_at	NP_061054	NM_018584
3.393	7.90	SCD	stearoyl-CoA desaturase (delta-9-desaturase)	211708_s_at	NP_005054	NM_005063
3.365	5.81	---	---	217027_x_at	---	---
3.361	5.81	FILIP1	filamin A interacting protein 1	1570515_a_at	NP_056502	NM_015687
3.350	14.16	---	---	241617_x_at	---	---
3.334	2.63	ARHGDIA	Rho GDP dissociation inhibitor (GDI) alpha	201167_x_at	NP_001172006	NM_001185077
3.310	10.22	SLC30A3	solute carrier family 30 (zinc transporter), member 3	207035_at	NP_003450	NM_003459
3.290	5.81	RPL14	ribosomal protein L14	219138_at	NP_001030168	NM_001034996
3.279	5.19	GPR56	G protein-coupled receptor 56	206582_s_at	NP_001139242	NM_001145770
3.212	0.00	CALR	calreticulin	200935_at	NP_004334	NM_004343
3.211	11.04	SCD	stearoyl-CoA desaturase (delta-9-desaturase)	211162_x_at	NP_005054	NM_005063
3.176	17.73	DPP4	dipeptidyl-peptidase 4	211478_s_at	NP_001926	NM_001935

3.149	4.52	DUSP7	dual specificity phosphatase 7	214793_at	NP_001938	NM_001947
3.130	13.03	WASF2	WAS protein family, member 2	224563_at	NP_001188333	NM_001201404
3.125	5.19	PDE7B	phosphodiesterase 7B	243438_at	NP_061818	NM_018945
3.113	4.52	ANXA1	Annexin A1	233011_at	NP_000691	NM_000700
3.100	4.52	ZFP36L2	zinc finger protein 36, C3H type-like 2	201367_s_at	NP_008818	NM_006887
3.082	0.00	FGF12	fibroblast growth factor 12	207501_s_at	NP_004104	NM_004113
3.055	4.68	CTSH	cathepsin H	202295_s_at	NP_004381	NM_004390
3.047	4.68	FAM189B	family with sequence similarity 189, member B	1555515_a_at	NP_001254537	NM_001267608
2.946	2.63	GSTT2	glutathione S-transferase theta 2	205439_at	NP_000845	NM_000854
2.943	7.24	FILIP1	filamin A interacting protein 1	1556325_at	NP_056502	NM_015687
2.925	4.52	DYRK1A	dual-specificity tyrosine-(Y)-phosphorylation regulated kinase 1A	211541_s_at	NP_001387	NM_001396
2.923	14.16	MGP	matrix Gla protein	238481_at	NP_000891	NM_000900
2.918	4.68	PTPN23	protein tyrosine phosphatase, non-receptor type 23	223149_s_at	NP_056281	NM_015466
2.911	5.81	VEGFB	vascular endothelial growth factor B	203683_s_at	NP_001230662	NM_001243733
2.887	7.90	AIF1L	allograft inflammatory factor 1-like	223075_s_at	NP_001172024	NM_001002260
2.873	10.22	CYTH3	cytohesin 3	243752_s_at	NP_004218	NM_004227
-2.294	12.17	TMEM35	transmembrane protein 35	219685_at	NP_067650	NM_021637
-2.299	13.03	ANGPTL4	angiopoietin-like 4	221009_s_at	NP_001034756	NM_001039667
-2.307	10.22	---	---	1558605_at	---	---
-2.311	15.63	MAP9	microtubule-associated protein 9	235550_at	NP_001034669	NM_001039580
-2.332	16.54	GATA6	GATA binding protein 6	210002_at	NP_005248	NM_005257
-2.332	14.16	PRSS3	protease, serine, 3	213421_x_at	NP_001184026	NM_001197097
-2.341	8.70	---	---	230820_at	---	---
-2.346	19.02	ADAM12	ADAM metallopeptidase domain 12	226777_at	NP_003465	NM_003474
-2.351	14.16	PRSS3	protease, serine, 3	207463_x_at	NP_001184026	NM_001197097
-2.366	17.73	ZFHX4	zinc finger homeobox 4	219779_at	NP_078997	NM_024721
-2.372	10.22	PSG7	pregnancy specific beta-1-glycoprotein 7 (gene/pseudogene)	205602_x_at	NP_001193579	NM_001206650
-2.377	11.04	PSG1	pregnancy specific beta-1-glycoprotein 1	208257_x_at	NP_001171754	NM_001184825
-2.378	14.16	MAP9	microtubule-associated protein 9	228423_at	NP_001034669	NM_001039580
-2.390	13.03	SUZ12P	Suppressor of zeste 12 homolog pseudogene	217704_x_at	---	NR_024187
-2.392	8.70	PCDHB16	protocadherin beta 16	232099_at	NP_066008	NM_020957
-2.406	12.17	LAMC2	laminin, gamma 2	207517_at	NP_005553	NM_005562
-2.412	16.54	IL8	interleukin 8	211506_s_at	NP_000575	NM_000584
-2.417	9.42	HINT3	histidine triad nucleotide binding protein 3	228697_at	NP_612638	NM_138571
-2.432	12.17	---	---	213747_at	---	---
-2.457	10.22	---	---	1560048_at	---	---
-2.460	12.17	TMEM163	transmembrane protein 163	223503_at	NP_112185	NM_030923
-2.486	19.02	GSTT1	glutathione S-transferase theta 1	203815_at	NP_000844	NM_000853
-2.498	10.22	CCDC122	coiled-coil domain containing 122	1553894_at	NP_659411	NM_144974
-2.507	13.03	CDKN2A	cyclin-dependent kinase inhibitor 2A	207039_at	NP_000068	NM_000077
-2.515	13.03	GLIPR1	GLI pathogenesis-related 1	204221_x_at	NP_006842	NM_006851
-2.522	9.42	EPG5	Ectopic P-granules autophagy protein 5 homolog (C. elegans)	1563471_at	NP_066015	NM_020964
-2.530	11.04	VLDLR	very low density lipoprotein receptor	209822_s_at	NP_001018066	NM_001018056
-2.539	14.16	OAS1	2'-5'-oligoadenylate synthetase 1, 40/46kDa	202869_at	NP_001027581	NM_001032409
-2.576	13.03	IL1A	interleukin 1, alpha	210118_s_at	NP_000566	NM_000575
-2.651	10.22	PSG4	pregnancy specific beta-1-glycoprotein 4	208191_x_at	NP_002771	NM_002780
-2.710	9.42	---	---	237372_at	---	---
-2.721	8.70	UHRF1BP1L	UHRF1 binding protein 1-like	213120_at	NP_001006948	NM_001006947
-2.743	8.70	PCDHB14	protocadherin beta 14	231726_at	NP_061757	NM_018934
-2.815	9.42	WDR78	WD repeat domain 78	1554140_at	NP_079039	NM_024763

-2.837	14.16	DDX6	DEAD (Asp-Glu-Ala-Asp) box helicase 6	1562836_at	NP_001244120	NM_001257191
-2.865	8.70	---	---	232535_at	---	---
-2.973	19.02	PNMA2	paraneoplastic Ma antigen 2	209598_at	NP_009188	NM_007257
-3.023	15.63	TTC29	tetratricopeptide repeat domain 29	223962_at	NP_114162	NM_031956
-3.041	14.16	EDIL3	EGF-like repeats and discoidin I-like domains 3	225275_at	NP_005702	NM_005711
-3.068	19.02	ADAM12	ADAM metallopeptidase domain 12	202952_s_at	NP_003465	NM_003474
-3.087	13.03	LPXN	leupaxin	216250_s_at	NP_001137467	NM_001143995
-3.254	10.22	LOC100289026	uncharacterized LOC100289026	237737_at	---	XR_110942
-3.336	15.63	HEY2	hairy/enhancer-of-split related with YRPW motif 2	219743_at	NP_036391	NM_012259
-3.387	10.22	LAMC2	laminin, gamma 2	202267_at	NP_005553	NM_005562
-3.454	16.54	GUCY1B3	guanylate cyclase 1, soluble, beta 3	203817_at	NP_000848	NM_000857
-3.522	14.16	ATP6V0D2	ATPase, H+ transporting, lysosomal 38kDa, V0 subunit d2	1553153_at	NP_689778	NM_152565
-4.267	15.63	CCDC81	coiled-coil domain containing 81	220389_at	NP_001149946	NM_001156474
-4.449	19.02	CYP1B1	cytochrome P450, family 1, subfamily B, polypeptide 1	202436_s_at	NP_000095	NM_000104
-5.208	15.63	CYP1B1	cytochrome P450, family 1, subfamily B, polypeptide 1	202435_s_at	NP_000095	NM_000104
-5.609	9.42	SERPIND1	serpin peptidase inhibitor, clade D (heparin cofactor), member 1	205576_at	NP_000176	NM_000185

Supplemental Table 7. Clinical characteristics of colorectal carcinoma patients subjected to immunohistochemical analysis of SPARCL1, CD31 and α-SMA expression. The patients were differentiated by GBP-1 expression. UICC stage, tumor, grading, age, and sex of both of the groups were closely matched and are given for each patient. Normal colon tissue was used from the same CRC patients in n=15 cases and was obtained at least 10 cm distant from the primary tumor. Normal colon from the cohort employed in Fig. 4C was used for n=5 patients due to small normal colon specimens from the corresponding CRC tissue. Chi square test and Mann-Whitney-U-test were used to analyze statistical differences (n.s.=not significant). This patient cohort was used in the stainings shown in Fig. 4A, 4B, 4D, 7 and, Supplementary Fig. 4 and 5.

Patients	GBP-1 tissue	UICC stage	Grading	Age	Sex
1	+	III	3	70	f
2	+	III	1	70	m
3	+	IV	1	66	f
4	+	III	3	64	m
5	+	III	1	69	m
6	+	I	1	75	m
7	+	III	3	60	m
8	+	III	2	23	m
9	+	I	1	81	m
10	+	I	1	59	m
11	+	III	1	75	m
12	+	III	3	75	m
13	-	I	2	59	m
14	-	I	1	64	f
15	-	I	3	71	m
16	-	II	3	57	f
17	-	IV	1	57	m
18	-	III	1	59	m
19	-	IV	1	76	f
20	-	III	3	78	m
21	-	II	1	67	m
22	-	IV	2	49	f
23	-	I	2	74	m
24	-	II	3	58	m
p-value		n.s.	n.s.	n.s.	n.s.

Supplemental Table 8. Clinical characteristics of the colorectal carcinoma patients included in the analysis of the comparison of SPARCL1 expression in normal colon and CRC (Fig. 4C) and the correlation analysis SPARCL1 and GBP-1 expression in CRC (Fig. 4E). CRC patients (n=127 [correlation analysis, Fig. 4E] and thereof n=42 [normal/tumor comparison, Fig. 4C]) were matched according to UICC stage. Distributions of UICC stages, grading, age, and sex are given.

Characteristics	Correlation Analysis (n=127), Fig. 3E	%	Normal/tumor comparison (n=42), Fig. 3C	%
Male:female ratio	74:53 = 1.39	NA	24:18 = 1.33	NA
Mean/range age (years)	65.0/22-90	NA	63.0/22-81	NA
Pathological stage (UICC 2009)				
I	33	26.0	11	26.2
II	36	28.3	11	26.2
III	30	23.6	8	19.0
IV	28	22.0	12	28.6
Histopathological grading				
Low grade (G_1/G_2)	86	67.7	28	66.7
High grade (G_3/G_4)	41	32.3	14	33.3

NA, not applicable.

Supplemetal references

1. Schaal, U., Grenz, S., Merkel, S., Rau, T.T., Hadjihannas, M.V., Kremmer, E., Chudasama, P., Croner, R.S., Behrens, J., Stürzl, M., et al. 2013. Expression and localization of axin 2 in colorectal carcinoma and its clinical implication. *Int J Colorectal Dis*.
2. Wolf, M.J., Adili, A., Piotrowitz, K., Abdullah, Z., Boege, Y., Stemmer, K., Ringelhan, M., Simonavicius, N., Egger, M., Wohlleber, D., et al. 2014. Metabolic activation of intrahepatic CD8+ T cells and NKT cells causes nonalcoholic steatohepatitis and liver cancer via cross-talk with hepatocytes. *Cancer Cell* 26:549-564.
3. Schellerer, V.S., Croner, R.S., Weinländer, K., Hohenberger, W., Stürzl, M., and Naschberger, E. 2007. Endothelial cells of human colorectal cancer and healthy colon reveal phenotypic differences in culture. *Lab Invest* 87:1159-1170.
4. Naschberger, E., Schellerer, V.S., Rau, T.T., Croner, R.S., and Stürzl, M. 2011. Isolation of endothelial cells from human tumors. *Methods Mol Biol* 731:209-218.
5. Naschberger, E., Croner, R.S., Merkel, S., Dimmler, A., Tripal, P., Amann, K.U., Kremmer, E., Brueckl, W.M., Papadopoulos, T., Hohenadl, C., et al. 2008. Angiostatic immune reaction in colorectal carcinoma: Impact on survival and perspectives for antiangiogenic therapy. *Int J Cancer* 123:2120-2129.
6. Grenz, S., Naschberger, E., Merkel, S., Britzen-Laurent, N., Schaal, U., Konrad, A., Aigner, M., Rau, T.T., Hartmann, A., Croner, R.S., et al. 2013. IFN-gamma-Driven Intratumoral Microenvironment Exhibits Superior Prognostic Effect Compared with an IFN-alpha-Driven Microenvironment in Patients with Colon Carcinoma. *Am J Pathol* 183:1897-1909.
7. Stürzl, M., Roth, W.K., Brockmeyer, N.H., Zietz, C., Speiser, B., and Hofschneider, P.H. 1992. Expression of platelet-derived growth factor and its receptor in AIDS-related Kaposi sarcoma in vivo suggests paracrine and autocrine mechanisms of tumor maintenance. *Proc Natl Acad Sci U S A* 89:7046-7050.
8. Chalmers, C.R., Fenwick, S.W., Toogood, G.J., and Hull, M.A. 2006. Immunohistochemical measurement of endothelial cell apoptosis and proliferation in formalin-fixed, paraffin-embedded human cancer tissue. *Angiogenesis* 9:193-200.